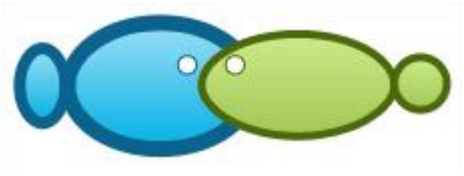

Preparation of collagen nanofibril-scaffold from the skin of catfish (*Pangasianodon hypophthalmus*) farmed in the Mekong Delta

[1]Quoc P. Ho, [2]Minh Thuy L. Thi, [1]Lien H. Huynh, [2]Minh P. Tran, [1]Bich Thuyen N. Thi, [3]Yasuaki Takagi

[1] College of Engineering Technology, Can Tho University, Can Tho City, Viet Nam;
[2] College of Aquaculture and Fisheries, Can Tho University, Can Tho City, Viet Nam;
[3] Faculty of Fisheries Sciences, Hokkaido University, 3-1-1 Minato-cho, Hakodate, Hokkaido 041-8611, Japan. Corresponding author: Q. P. Ho, hqphong@ctu.edu.vn

Abstract. Type I collagen with high purity and high denaturation temperature was successfully extracted from the skin of catfish, *Pangasianodon hypophthalmus* farmed in the Mekong Delta. The effects of the phosphate buffer (PB) concentration, pH, NaCl concentration, incubation temperature of the reaction fluid, and nHA content on the formation of the collagen-nanofibril scaffold were clarified. BP concentration and NaCl concentration had a significant effect on the nanofibril diameter of the scaffold and the mean diameters of the SC nanofibrils are reaching 98 nm and 109 mm corresponding to 90 mM PB and 140 mM NaCl, respectively. The pH also affected the morphology of the scaffold but not the nanofibril diameter of the scaffold. The diameter of collagen fibrils increases with increasing incubation temperature and the collagen fibrils become particle-like at the temperature of 37°C. nHA content will change the diameter of the collagen fibrils and it is disappeared when nHA to collagen weight ratios are 1/10 and 1/15. Overall results suggested that collagen-nanofibril scaffolds could be prepared in conditions of 60 mM PB, 1 mg mL^{-1} collagen, pH 7.4, 93 mM NaCl, the incubation temperature 25 °C, and nHA to collagen weight ratio of 1/15.
Keywords: collagen fibrils, collagen self-assembly, *P. hypophthalmus*, scaffold, type I collagen.

Introduction. Bioscaffolds, known as artificial architecture for biosynthetic extracellular matrix (ECM), are used to create a 3D environment for the formation of the 3D structure of the tissue. Several properties are essential for the design of an ideal scaffold including biocompatibility, biodegradability, bioresorbability, porous structure, and good mechanical strength. Natural polymers such as collagen, silk, fibrin, and chitosan were usually utilized to prepare the scaffold because of their biocompatible properties (Thomas et al 2007; Venugopal et al 2008; Zhuang et al 2007). However, the mechanical properties of these natural polymers were very weak. They must be modified by reinforced materials to apply for tissue engineering (Wei & Ma 2004). The reinforced materials made from calcium phosphate, ceramic, and bioglass were usually applied to modify to enhance not only mechanical properties but also the biocompatible properties of these natural polymers (Chen & Liu 2016).

One of the calcium phosphate forms is hydroxyapatite (HA) which is usually used to enhance the stiffness of the polymer. HA particles can be synthesized from pure chemicals by numerous methods such as mechanochemistry, ultrasonic and microwave, sol-gel, chemical precipitation, hydrothermal method, hydrolysis, and microemulsion (Barakat et al 2008). However, recently, many studies have focused on extracting natural HA from fish bone (Boutinguiza et al 2012; Piccirillo et al 2014), bovine bone (Barakat et al 2009), and fish scale (Huang et al 2011) since research carried out so far indicates that these natural resources can be a potential alternative to Ca and P precursor for the production of phase-pure and thermally stable HA (Akram et al 2014).

Type I collagen is widely used in food, cosmetics, pharmaceutical, and biomedical industries. In the biomedical field, collagen is fabricated as cellular scaffolds in tissue

engineering (Kim & Mendis 2006; Benjakul et al 2012; Al-Nimry et al 2021). One of the critical properties of type I collagen for biomedical applications is its ability to self-assemble into nanofibrils, the standard form of collagen in the animal body. Fibrous collagen has better properties, such as being more durable and difficult to denature than soluble collagen (Tiktopulo & Kajava 1998). Moreover, the nanofibril morphology, especially its diameter and alignment, greatly affected the growth and differentiation of cells when used as scaffolds (Christopherson et al 2009; Moroi et al 2019). Therefore, the fabrication of collagen into nanofibril structures and the regulation of their morphology are of great interest. Pilot studies using type I collagen have shown that the pH, ionic strength, and divalent anion concentration of the fibril-formation fluid influence the process of nanofibril formation and morphology of the produced nanofibrils (Li et al 2009; Harris et al 2013).

The major sources of type I collagen are mammals, including bovine skin and tendon, porcine skin, and rat tail (Parenteau-Bareil et al 2010). However, recent studies suggested that the skin, swim bladder, and scales of fishes are potential alternative sources for type I collagen production (Kim et al 2012; Liu et al 2012; Kaewdang et al 2014; Wang et al 2014; Kittiphattanabawon et al 2015). Catfish (*Pangasianodon hypophthalmus*) is one of eleven species of *Pangasianodon* that live in the Mekong River. This fish grows relatively fast and reaches 1.5-3 kg after 1-2 years of raising in ponds. In recent years, catfish farm has developed strongly in the Mekong Delta, Vietnam. The yield of catfish was 1.2 million tons in 2012 and reached 1.42 million tons in 2018 with an export value of 2.6 billion USD (VASEP 2019). With the high economic value that catfish brings, the farming and processing of it have been expanding dramatically, leading to producing a huge number of byproducts such as fat, bone, and skin.

In this study, byproducts such as bone and skin of catfish were applied to produce collagen-nanofibril scaffolds. Important factors affecting the formation of collagen nanofibril scaffolds such as the phosphate buffer concentration, pH, NaCl concentration, and temperature of the reaction fluid and HA content will be investigated.

Material and Method. Bone and skin of catfish were provided by a local fish-fillet processing factory in Can Tho, Vietnam. Pepsin (from porcine gastric mucosa) 0.7 fip-u mg^{-1}, Na_2HPO_4, NaH_2PO_4, HCl, NaCl and dialysate bag were supplied by Merck (Vietnam). The experiments were carried out from January 2021 to March 2022.

Preparation of hydroxyapatite from catfish bone. Nanoydroxyapatite (nHA) was prepared from bone of catfish following the previous report with little modification (Ho et al 2020). Catfish bone was first cooked at 100°C for 24 h to remove tissue, then dried at 80-100°C for 24 h. After pretreatment with 0.1 M NaOH for 24 h and washed with water, the pretreated bone was then calcined at 900°C for 6 h in a furnace (Nabertherm, LHT 1750°C) to remove all organic components in the bone. The calcined bovine bone was then grinded into powder with particle sizes of 5 to 10 µm by using high speed ball mill.

Catfish bone power (CBP) was dissolved in 50 mL of 1 M H_3PO_4 to form homogeneous mixture and then it was reacted with $Ca(OH)_2$ aqueous solution to obtain a Ca/P ratio of 1.67. After 2 h of reaction at 40°C, the mixture was adjusted to room temperature and aged for 24 hours before centrifugation. The precipitate was washed several times with distilled water, dried at 100°C and calcined for 4h at 1000°C to obtain nHA.

Collagen extraction. Collagen extraction and purification were conducted as following the report of Singh et al (2011). Briefly, the catfish skin was washed with distilled water, cut into pieces (about 2 cm x 2 cm) and then treated in 0.1 M NaOH solution at a skin/solution ratio of 1:10 g/mL for 6 h at a stirring speed of 300 rpm (the NaOH solution was changed every 2 h to increase the removal of minerals and fats). After the treatment with NaOH, the samples were washed with distilled water to neutral pH and subsequently with ethanol (99.5%) at the ratio of 1:10 g mL^{-1} for 24 h with 300 rpm stirring. All procedures were conducted at 4°C.

The pretreated samples were cut into 0.5 cm x 0.5 cm pieces and were extracted in pH 2.0 HCl aqueous solution containing 1% pepsin with a sample/solution ratio of 1:40

at a stirring speed of 300 rpm for 24 hours. After the filtration using a polyester filter cloth, the solution was salted-out by adding NaCl to a final concentration of 1.0 M. The precipitate was obtained by centrifugation at 9000×g for 20 min and re-dissolved in HCl solution (pH 2.0) with a precipitate/solution ratio of 1:20. Then, the sample was dialyzed in a dialysis tube (molecular cut off 14,000 kDa, Sigma-Aldrich) using distilled water for 24 hours at a stirring speed of 400 rpm. The distilled water was changed every 4 hours. After 24 hour-dialysis, the obtained collagen solution was freeze-dried. The extraction and purification processes were carried out at 4^{o}C to avoid collagen denaturation. The percentage of the dry weight of collagen extracted compared to the wet weight of the initial tissues was calculated as the collagen yield.

Preparation of collagen-nanofibril scaffold. Collagen fibrils were fabricated according to the procedure as shown in Figure 1. The freeze-dried collagen extracted from catfish skin was dissolved in HCl aqueous solution (pH 2.0) to prepare the homogeneous collagen solution at 4^{o}C. Phosphate buffer was prepared by mixing two sodium phosphates $Na_2HPO_4.12H_2O$ and $NaH_2PO_4.2H_2O$ and its pH value could be adjusted by changing the ratio between them. Nanohydroxyapatite obtained from previous work was dispersed into phosphate buffer (PB) and then mixed with the collagen solution at a collagen solution to BP solution ratio of 1:2. The mixture was added to 12 well plates for 60 minutes before it was dehydrated by applying a gradient of ethanol concentrations from 30 to 99.5% (10 min for each concentration) at room temperature. Tert-butanol was then replaced ethanol and the drying process was completed by using freeze dryer at -40^{o}C for 48 hours to form collagen nanofibril-scaffold. The factors that affected the nanofibril formation, such as PB concentration, pH of the PB, NaCl concentration, nHA content and incubation temperature were studied.

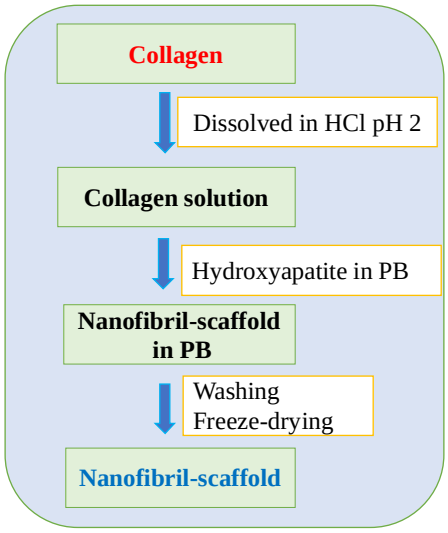

Figure 1. The preparation procedure of collagen nanofibril-scaffold.

Characterization methods

Fourier-transform infrared spectroscopy (FT-IR). FT-IR device (Thermo Scientific Nicolet 6700 FT-IR Spectrometer, USA) was used to evaluate important functional groups of collagen fibrils. The spectra were recorded from 4000 to 400 cm^{-1} with a data acquisition rate of 1 cm^{-1} per point. The resulting spectra were analyzed by using OMINIC software.

Sodium dodecyl sulfate-polyacrylamide gel electrophoresis (SDS-PAGE). SDS-PAGE was performed according to the method of Laemmli (1970). The lyophilized collagens were dissolved in the HCl aqueous solution (pH 3.0, 1 mg collagen mL^{-1}) and then mixed at a ratio of 1:1 (v/v) with sample buffer (0.5 M Tris–HCl buffer, pH 6.8, with 4% SDS and 10% sucrose) containing 10% β-mercaptoethanol. The mixed solution was boiled for 3 min. Ten microliters of the mixture was loaded onto each lane. Electrophoresis was performed at 14 mA for the stacking gel and 24 mA for the 10% running gel. After

electrophoresis, the gel was stained for 30 min with a 0.1% Coomassie Brilliant Blue R250 solution and destained with a mixture of 20% ethanol, 5% acetic acid, and 2.5% glycerin. Precision Plus Protein All Blue Standards (Bio-Rad Laboratories, Inc., Hercules, CA, USA) was used to estimate the molecular weight.

Circular dichroism (CD) analyses. CD spectra were measured using a JASCO model 725 spectrometer (JASCO, Tokyo, Japan). The measurement was performed following the method of Ikoma et al (2003) with some modifications. Lyophilized collagens were dissolved in an HCl aqueous solution (pH 3.0) to 0.1 mg mL^{-1} and placed into a quartz cell. CD spectra were measured at 190–250 nm wavelengths at 10°C under a scan speed of 50 nm min^{-1} with an interval of 0.1 nm. The rotatory angle at a fixed wavelength of 221 nm was then measured at 20-45°C with a rate of 1°C min^{-1} to determine the denaturation temperature of the collagen molecules.

UV analysis. After mixing the collagen solution and PB solution, time-dependent changes in UV absorption at 320 nm were measured using an ultraviolet spectrophotometer (Thermo Evolution 160 UV-VIS, Thermo Fisher Scientific, Waltham, MA, USA).

Field emission scanning electron microscopy (FE-SEM). The collagen nanofibril scaffolds were fabricated according to the procedures described above. The morphology of collagen nanofibrils was observed by field emission scanning electron microscopy (FE-SEM; S-4800, Hitachi High-Tec GLOBAL, Tokyo, Japan) with an acceleration voltage of 30 kV. The samples were coated with platinum before being subjected to FE-SEM. The diameter of nanofibrils was determined by using ImageJ software through FE-SEM images.

Statistical analyses. Student's *t*-test was used to compare the fibril diameters and executed by Origin software®.

Results and Discussion

Preparation of nanohydroxyapatite from fish bone. The nHA product and commercial HA purchased from Merck (Figure 2) were characterized by XRD diffraction. The results showed that the samples existed with characteristic peaks of HA at 2θ at 10.8°, 21,8°, 25.9°, 28.9°, 31.9°, 32.2°, 32.9°, 34.1°, 39.8°, 46.7°, 48.1°, 49.5°, 50.6°, 51.3°, 52.1° and 53.2° and these diffraction peaks match with HA standard card ICDD (International Center for Diffraction Data) (01-080-6199). In addition, FE-SEM image showed that the HA product has nanorod shape with a diameter of 36.7±12.6 nm and 76.9±22 nm long (Figure 2b). It can be stated that HA was successfully prepared from catfish bone.

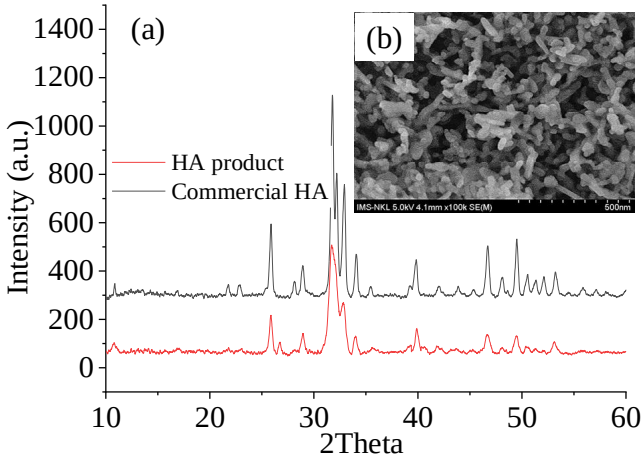

Figure 2. XRD diffraction of nHA (a) and SEM image of nHA (b). Reaction condition: CBP 25 g L^{-1}, 1M H_3PO_4, pH 11, reaction temperature 40°C and calcined temperature 600 °C for 4 hours, Ca/P = 1.67.

Preparation and characterization of collagen molecules. The collagen extraction yield of catfish skin was 22.4%. The SDS-PAGE patterns of collagens (Figure 3a) showed that skin collagen (SC) had two α-chains (approximately 120 kDa and 130 kDa) as the major constituents, indicating that the collagen was type I. Moreover, SC was highly purified because there were no low-molecular-weight bands. The CD analyses (Figures 3c-d) clarifies that SC showed a rotatory maximum at 221 nm and a crossover point (zero rotation) at about 212 nm, indicating that collagen retained triple helical structure. When the temperature rose, the CD [221] values started rapid decrease at about 34°C for SC due to the decomposition of the collagen triple helical structure. Denaturation temperature (Td), determined as the temperature with the fastest decreased speed of the CD [221] value, was 35.5°C for SC. The FTIR analysis (Figure 3b) showed the characteristic absorption peaks of collagen at wavelengths 3284 cm^{-1}, 2927 cm^{-1}, 1650 cm^{-1}, 1550 cm^{-1}, and 1370 cm^{-1}, corresponding to amide A, amide B, amide I, amide II, and amide III, respectively (Singh et al 2011). It can be stated that collagen type I was successfully extracted from catfish skin with high efficiency and purity.

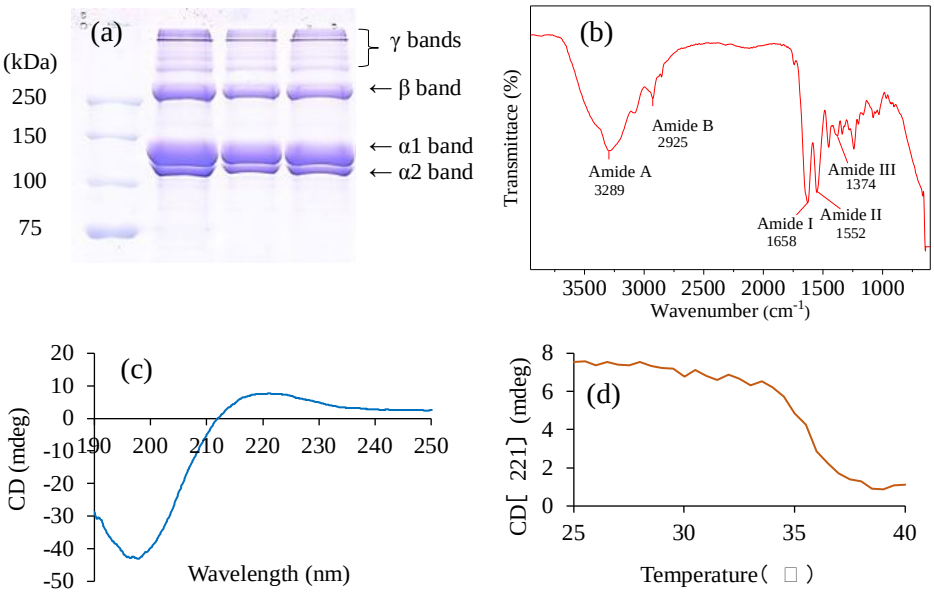

Figure 3. Characterization of the extracted collagen molecules: SDS-PAGE (a), FTIR (b) and CD (c, d).

Preparation of collagen-nanofibril scaffold. Formation of collagen fibrils was believed to be a self-assembled process of collagen molecules in solution when it was distributed in suitable conditions such as phosphate buffer or changing ionic factors, temperature, and concentration (Bae et al 2009; Zhang et al 2014; Zhu & Kaufman 2014). It is also known that the fibril formation goes through three phases: lag, growth, and plateau. In the initial stage (lag phase), several collagen molecules are staggeredly arranged to form nuclei, and they subsequently aggregate linearly to form subfibrillar units. Then, the lateral aggregation of subfibrillar units undergoes the growth phase to form collagen-nanofibril scaffold (Trelstad et al 1976; Christiansen et al 2000; Meng et al 2020), which can be monitored as an increase in the turbidity of the solution. The optical density (OD) values were used to describe formation process of collagen-nanofibril scaffold in this study.

Effect of concentration of phosphate buffer on collagen-nanofibril scaffold. To investigate the effects of PB concentrations on the formation of collagen-nanofibril scaffold, the experiments were conducted with PB concentrations at 15-90 mM (Figure 4). At 15 and 30 mM PB, the OD of the SC solution (Figure 4a) increased rapidly during the first 5 min and quickly reached the plateau phase after that. At 60 mM PB, the first 5-min OD increase was smaller than at 15 and 30 mM PB, and the gradual OD increase was

followed, reaching the plateau phase till 60 min. At 90 mM PB, the OD increased slowly and did not reach the plateau phase within 60 min. The highest OD was observed in the 60 mM PB group, followed by the 30 mM and 15 mM groups, and the lowest OD was observed in the 90 mM PB group.

The FE-SEM results (Figures 4b-e) showed that the nanofibrils of the scaffold had a uniform diameter at 60 mM PB, while the nanofibril diameters showed significantly different at 90 mM PB. The nanofibril diameters were 62±12 nm, 67±10 nm, and 98±11 nm corresponding to 30 mM PB, 60 mM PB, and 90 mM PB, respectively. Nanofibrils were fused at 15 mM PB therefore the diameter was unmeasurable. This can be explained by the influence of phosphate ions on the interaction between bonds of collagen molecules. At low buffer concentrations, there is not enough ion to form fibrils but at high buffer concentrations, it causes adjacent fibrils to combine into larger size and reduces the amount of collagen fibrils (Pogany et al 1994; Uquillas et al 2011). From the results, the buffer concentration of 60 mM was selected as the condition to produce collagen-nanofibril scaffold.

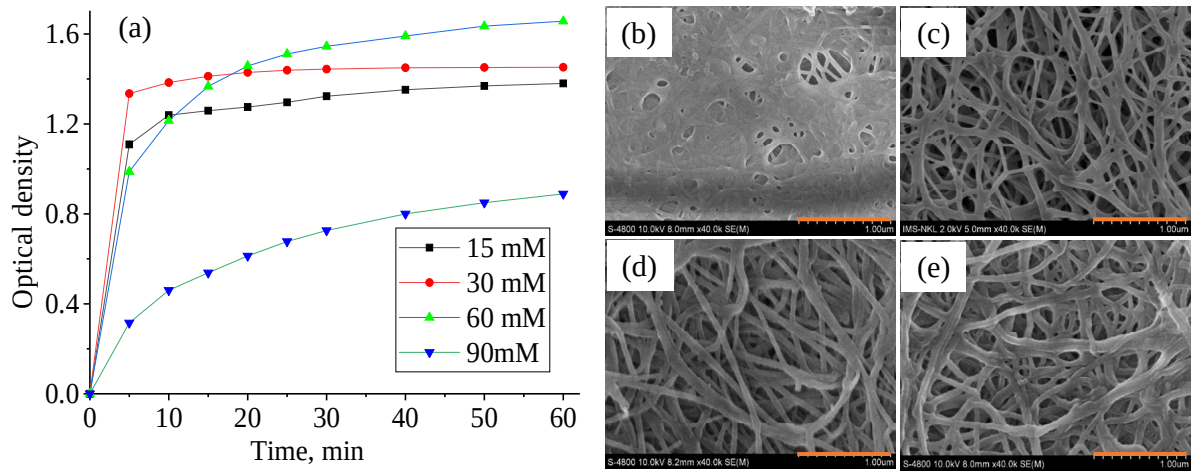

Figure 4. Optical density of collagen solutions formed in different phosphate buffer concentrations (a), and SEM images of collagen-nanofibril scaffolds: 15 mM (b), 30 mM (c), 60 mM (d), and 90 mM (e). Reaction conditions: pH 7.4, 1 mg mL^{-1} collagen, without NaCl, without nHA and the incubation time of 60 min at 25°C. Scale bars: 1 µm.

Effect of pH of phosphate buffer on collagen-nanofibril scaffold. To investigate the effect of pHs on formation of collagen-nanofibril scaffold, pH of the buffer solution was varied from 6.8 to 8.5. The UV scanning results of SC solutions are shown in Figure 5. The highest 5-min OD in the SC solutions was observed when the pH was 8.5, followed by pH 6.8, 7.4 and 7.9 groups. The OD in the pH 8.5 group reached the plateau phase soon after 5 min, whereas ODs of pH 6.8, 7.4 and 7.9 groups gradually increased and reached the plateau phase after 30 min. The FE-SEM images of collagen-nanofibril scaffolds showed that the nanofibrils are uniform at pH 7.4 (Figures 5c) with nanofibril diameters of 67±10 nm. At pH 6.8, 7.9, and 8.5, some SC nanofibrils showed slightly larger diameters, and the diameter variations became bigger (Figures 5b, d, e). The nanofibril diameters were 85±14 nm, 86±11 nm, and 88±11 nm corresponding to pH 6.8, 7.9, and 8.5, respectively. Collagen-nanofibril scaffold is formed when the pH is lower or higher than the isoelectric point (pI) of collagen (pI of collagen 5.1-7.6 (Park et al 2012)) and it strongly takes place at neutral pH. Some studies also showed that the formation of collagen fibrils was attributed to the binding of phosphate ions with collagen at the pI (Foegeding et al 1996) and this is consistent with the results obtained from this study in which pH 7.4 is the best condition to form a collagen-nanofibril scaffold.

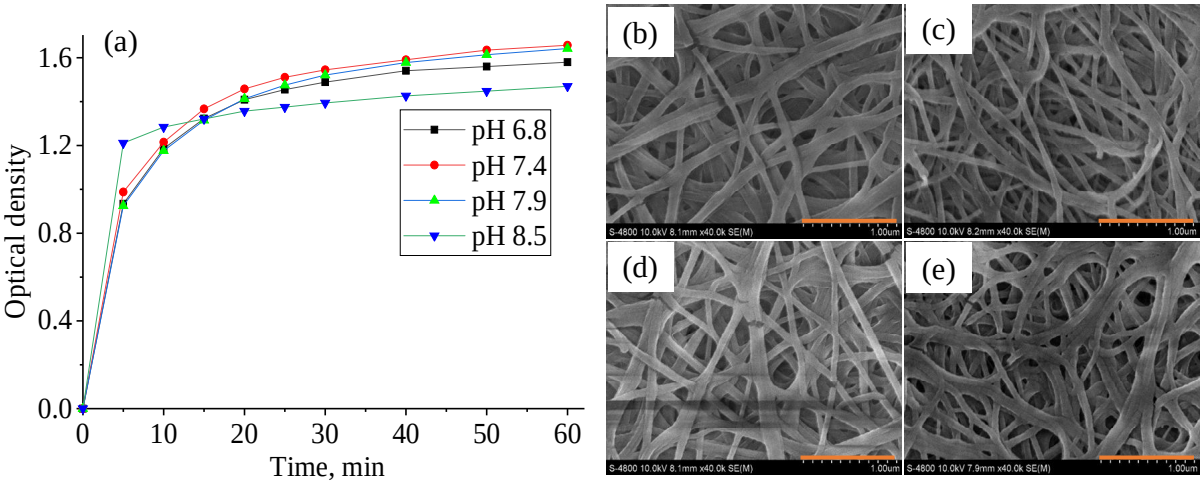

Figure 5. Optical density of collagen solutions formed in formed in the different pHs (a), and SEM images of collagen-nanofibril scaffolds: pH = 6.8 (b), pH = 7.4 (c), pH = 7.9 (d) and pH = 8.5 (e). Reaction conditions: 60 mM PB, 1 mg mL^{-1} collagen, without NaCl, without nHA and the incubation time of 60 min at 25°C. Scale bars: 1 µm.

Effect of NaCl concentration on collagen-nanofibril scaffold. Concentration of NaCl was varied from 0 mM to 140 mM to investigate its effect on the formation of collagen-nanofibril scaffold. The UV results (Figure 6a) showed that, with NaCl in the solution, OD of SC solutions increased slowly in 0-20 min and then rapidly increased from 20-60 min. The highest OD was observed when the NaCl concentration was 93 mM, followed by the 0 mM and 140 mM groups, while the 23 mM group was the lowest. The FE-SEM images showed that collagen nanofibrils of the scaffolds were formed in any conditions tested in this experiment (Figures 6b-e). The nanofibril diameter became thick when the NaCl concentration was 140 mM (Figure 6e). The concentrations of NaCl had the most important effect on nanofibril diameter among the examined factors. The effect was not linear at 0-93 mM NaCl with the mean nanofibril diameters were 67±10 nm, but it increased to 109±12 nm when the NaCl concentration was increased to 140 mM. These results are consistent with a study on fibrillar scaffold prepared from red stingray collagen (Bae et al 2009).

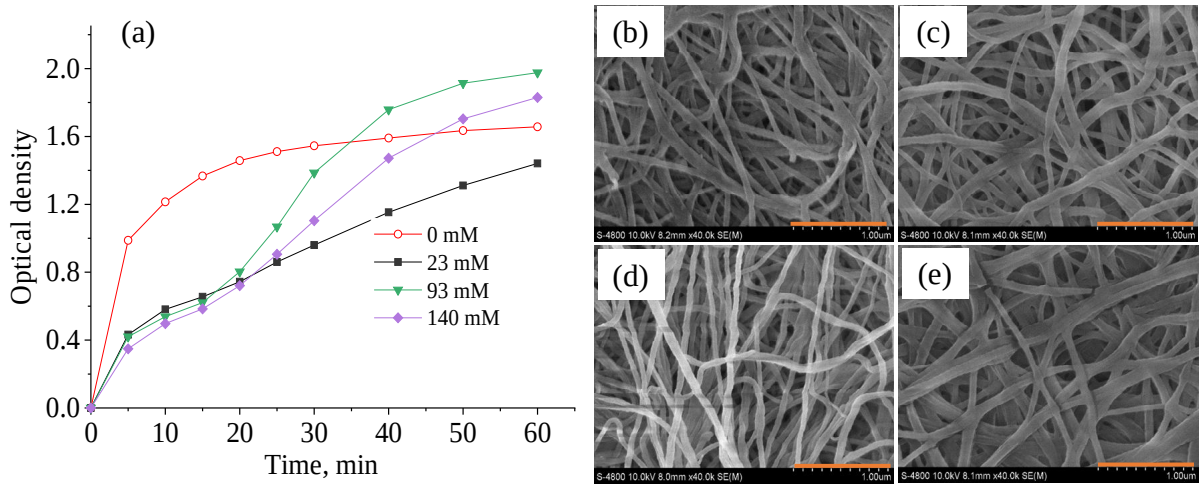

Figure 6. Optical density of collagen solutions formed in different NaCl concentrations (a), and SEM images of collagen-nanofibril scaffolds: 0 mM (b), 23 mM (c), 93 mM (d) and 140 mM (e). Reaction conditions: 60 mM PB, 1 mg mL^{-1} collagen, pH 7.4, without nHA, and the incubation time of 60 min at 25°C. Scale bars: 1 µm.

Effect of temperature on collagen-nanofibril scaffold. Experiments were carried out at different temperatures varied from 20 to 37°C to study the formation of the collagen-nanofibril scaffold. The UV results (Figure 7a) showed that at 20°C and 25°C, OD of SC

solutions increased slowly in 0-40 min and then rapidly increased from 40-60 min while at 30°C and 37°C, OD of SC solutions increased slowly in 0-20 min and then rapidly increased from 20-60 min. The lowest OD of the solution was observed at 20°C. It should be noted that the self-assembly of type I collagen was highly dependent on entropy or temperature (Kadler et al 1987). As entropy increased, the water molecules bound on the collagen surface began to dissociate causing collagen molecules in the solution to assemble into nanofibrils.

Moreover, the movement of collagen in the solution also depends on temperature. Low temperature (low entropy) means slow movement of collagen molecules in solution hence the formation of fibrils is also slow. In contrast, higher temperature (higher entropy) resulted in the higher movement of collagen molecules, which reduced the formation of nanofibrils (Parkinson et al 1995). FE-SEM images (Figures 7b-e) showed that at low temperature with a low rate of fibril formation, the structure of fibrils was not good and at high temperature, the quality of the fiber was also not good, especially when the temperature was 37°C, the fibrils formed were large and some were particle-like, instead of fibrils (Figure 7e). Therefore, an optimum formation temperature of the collagen-nanofibril scaffold was found to be 25°C in this study.

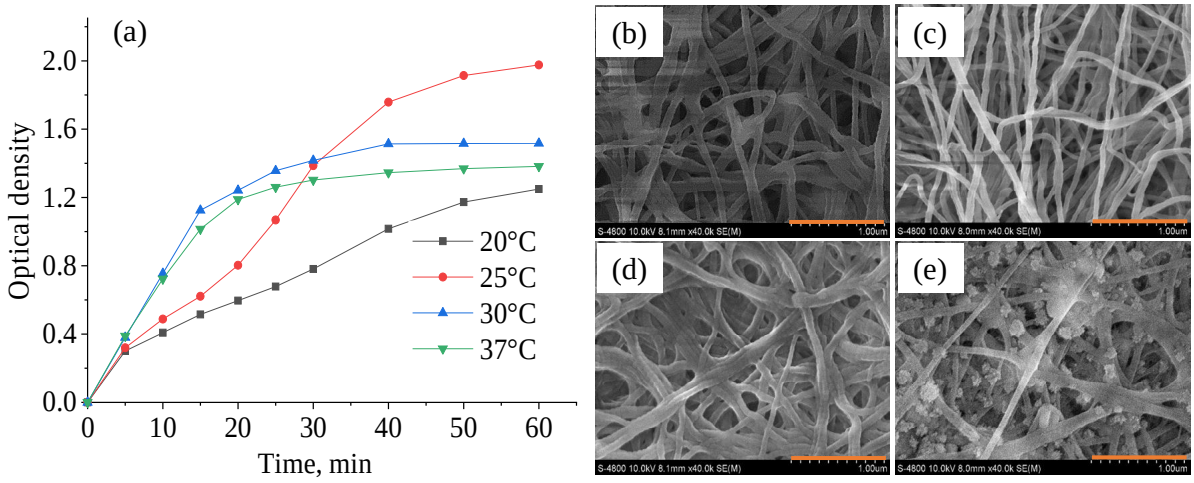

Figure 7. Optical density of collagen solutions formed in different temperature (a) and SEM images of collagen nanofibrils: 20°C (b), 25°C (c), 30°C (d), 37°C (e). Reaction conditions: 60 mM PB, 1 mg mL^{-1} collagen, pH 7.4, 93 mM NaCl, without nHA and the incubation time of 60 min. Scale bars: 1 μm.

Effect of HA content on collagen-nanofibril scaffold. The collagen-nanofibril scaffold is a highly porous structure that can be used as a good scaffold for cell culture. However, the mechanical properties of the scaffold are usually low and nHA was used as filler to improve its mechanical strength. In this study, nHA to collagen weight ratios were varied to investigate the influence on the formation of the collagen-nanofibril scaffold. The scaffolds formed are in a cylindrical shape and the HA content does not significantly change the outer structure (Figures 8a-d); however, nHA content significantly affects their mechanical properties, and the compressive strength of the scaffold increased with increasing the nHA content. In addition, FE-SEM images (Figures 8e-h) also presented that when the nHA content increased, the size of collagen fibrils increased. The nanofibril diameters increased from 68±10 to 126±28 nm at nHA to collagen weight ratio of 1/15 whereas collagen fibrils almost disappeared when the ratios were 1/10 and 1/5 (Figures 8g, h); which means that the porosity of the scaffold was significantly reduced. This suggests that the nHA to collagen weight ratio of 1/15 is suitable to prepare a collagen-nanofibril scaffold.

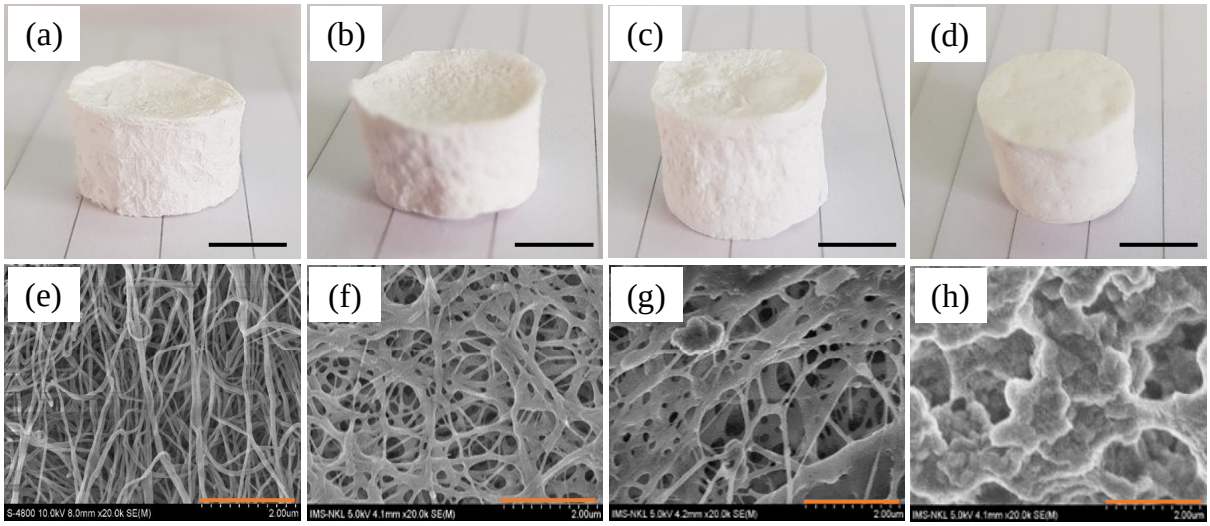

Figure 8. Optical images of collagen-nanofibril scaffolds (a-d) and SEM images of the collagen-nanofibril scaffolds (e-h). nHA to collagen weight ratio: without nHA (a, e), 1/15 (b, f), 1/10 (c, g) and 1/5 (d, h). Reaction conditions: 60 mM PB, 1 mg mL^{-1} collagen, pH 7.4, 93 mM NaCl, and the incubation time of 60 min at 25°C. Scale bars: 1 cm for optical images and 2 μm SEM images.

Conclusions. This study showed that type I collagen with high purity and high denaturation temperature was successfully extracted from the skin of catfish so it can be applied to prepare bioscaffolds. Moreover, the experiment also showed that the PB concentration, NaCl concentration, incubation temperature, and nHA content were the critical factors for the formation of the collagen-nanofibril scaffold. The suitable collagen-nanofibril scaffold can be prepared in conditions of 60 mM PB, 1 mg mL^{-1} collagen, pH 7.4, 93 mM NaCl, the incubation temperature 25°C, and nHA to collagen weight ratio of 1/15. With an annual yield of thousands of tons in the Mekong Delta, the catfish skin could be considered an important source to produce collagen-nanofibril scaffold for biomedical applications.

Acknowledgements. This study is funded in part by the Can Tho University Improvement Project VN14-P6, Grand No. F4-4, supported by a Japanese ODA loan.

Conflict of interest. The authors declare that there is no conflict of interest.

References

Al-Nimry S., Dayah A. A., Hasan I., Daghmash R., 2021 Cosmetic, biomedical and pharmaceutical applications of fish gelatin/hydrolysates. Marine Drugs 19(3):145.

Akram M., Ahmed R., Shakir I., Ibrahim W. A. W., Hussain R., 2014 Extracting hydroxyapatite and its precursors from natural resources. Journal of Materials Science 49:1461-1475.

Bae I., Osatomi K., Yoshida A., Yamaguchi A., Tachibana K., Oda T., Hara K., 2009 Characteristics of a self-assembled fibrillar gel prepared from red stingray collagen. Fisheries Science 75(3):765-770.

Barakat N. A. M., Khalil K. A., Sheikh F. A., Omran A. M., Gaihre B., Khil S. M., Kim H. Y., 2008 Physiochemical characterizations of hydroxyapatite extracted from bovine bones by three different methods: extraction of biologically desirable HAp. Materials Science and Engineering: C 28(8):1381-1387.

Barakat N. A. M., Khil M. S., Omran A. M., Sheikh F. A., Kim H. Y., 2009 Extraction of pure natural hydroxyapatite from the bovine bones bio waste by three different methods. Journal of Materials Processing Technology 209(7):3408-3415.

Benjakul S., Nalinanon S., Shahidi F., 2012 Fish collagen. In: Food biochemistry and food processing. 2nd edition. Simpson B. K. (ed), Wiley-Blackwell, Oxford, pp. 365-387.

Boutinguiza M., Pou J., Comesaña R., Lusquiños F., de Carlos A., León B., 2012 Biological hydroxyapatite obtained from fish bones. Materials Science and Engineering: C 32(3):478-486.

Chen F. M., Liu X., 2016 Advancing biomaterials of human origin for tissue engineering. Progress in Polymer Science 53: 86-168.
Christiansen D. L., Huang E. K., Silver F. H., 2000 Assembly of type I collagen: fusion of fibril subunits and the influence of fibril diameter on mechanical properties. Matrix Biology 19(5):409-420.
Christopherson G. T., Song H., Mao H. Q., 2009 The influence of fiber diameter of electrospun substrates on neural stem cell differentiation and proliferation. Biomaterials 30(4):556-564.
Foegeding E. A., Lanier T. C., Hultin H. O., 1996 Characteristics of edible muscle tissues. In: Food chemistry. Fennema O. R. (ed), Marcel Dekker Inc., New York, pp. 902-906.
Harris J. R., Soliakov A., Lewis R. J., 2013 *In vitro* fibrillogenesis of collagen type I in varying ionic and pH conditions. Micron 49:60-68.
Ho Q. P., Tao T. D., Huynh L. H., Wang M. J., 2020 Biocomposite scaffold preparation from hydroxyapatite extracted from waste bovine bone. Green Processing and Synthesis 9(1):37-47.
Huang Y. C., Hsiao P. C., Chai H. J., 2011 Hydroxyapatite extracted from fish scale: effects on MG63 osteoblast-like cells. Ceramics International 37(6):1825-1831.
Ikoma T., Kobayashi H., Tanaka J., Walsh D., Mann S., 2003 Physical properties of type I collagen extracted from fish scales of *Pagrus major* and *Oreochromis niloticus*. International Journal of Biological Macromolecules 32(3-5):199-204.
Kadler K. E., Hojima Y., Prockop D. J., 1987 Assembly of collagen fibrils de novo by cleavage of the type I pC-collagen with procollagen C-proteinase. Assay of critical concentration demonstrates that collagen self-assembly is a classical example of an entropy-driven process. Journal of Biological Chemistry 262(32):15696-15701.
Kaewdang O., Benjakul S., Kaewmanee T., Kishimura H., 2014 Characteristics of collagens from the swim bladders of yellowfin tuna (*Thunnus albacares*). Food Chemistry 155:264-270.
Kim H. K., Kim Y. H., Kim Y. J., Park H. J., Lee N. H., 2012 Effects of ultrasonic treatment on collagen extraction from skins of the sea bass *Lateolabrax japonicus*. Fisheries Science 78(2):485-490.
Kim S. K., Mendis E., 2006 Bioactive compounds from marine processing byproducts – a review. Food Research International 39(4):383-393.
Kittiphattanabawon P., Benjakul S., Sinthusamran S., Kishimura H., 2015 Characteristics of collagen from the skin of clown featherback (*Chitala ornata*). International Journal of Food Science and Technology 50(9):1972-1978.
Laemmli U. K., 1970 Cleavage of structural proteins during assembly of head of bacteriophage T4. Nature 227(5259):680-685.
Li Y., Asadi A., Monroe M. R., Douglas E. P., 2009 pH effects on collagen fibrillogenesis *in vitro*: electrostatic interactions and phosphate binding. Materials Science and Engineering: C 29(5):1643-1649.
Liu D., Liang L., Regenstein J. M., Zhou P., 2012 Extraction and characterisation of pepsin-solubilised collagen from fins, scales, skins, bones and swim bladders of bighead carp (*Hypophthalmichthys nobilis*). Food Chemistry 133(4):1441-1448.
Meng D., Li W., Ura K., Takagi Y., 2020 Effects of phosphate ion concentration on *in-vitro* fibrillogenesis of sturgeon type I collagen. International Journal of Biological Macromolecules 148:182-191.
Moroi S., Miura T., Tamura T., Zhang X., Ura K., Takagi Y., 2019 Self-assembled collagen fibrils from the swim bladder of Bester sturgeon enable alignment of MC3T3-E1 cells and enhance osteogenic differentiation. Materials Science and Engineering: C 104:109925.
Parenteau-Bareil R., Gauvin R., Berthod F., 2010 Collagen-based biomaterials for tissue engineering applications. Materials 3(3):1863-1887.
Park S. H., Song T., Bae T. S., Khang G., Choi B. H., Park S. R., Min B. H., 2012 Comparative analysis of collagens extracted from different animal sources for application of cartilage tissue engineering. International Journal of Precision Engineering and Manufacturing 13(11):2059-2066.
Parkinson J., Kadler K. E., Brass A., 1995 Simple physical model of collagen fibrillogenesis based on diffusion limited aggregation. Journal of Molecular Biology 247(4):823-831.

Piccirillo C., Pullar R. C., Tobaldi D. M., Castro P. M. L., Pintado M. M. E., 2014 Hydroxyapatite and chloroapatite derived from sardine by-products. Ceramics International 40(8):13231-13240.
Pogany G., Hernardez D. J., Vogel K. G., 1994 The *in vitro* interaction of proteoglycans with type I collagen is modulated by phosphate. Archives of Biochemistry and Biophysics 313(1):102-111.
Report on Vietnam's *Pangasius*, 2019. Available at: https://vasep.com.vn/san-pham-xuat-khau/ca-tra/tong-quan-nganh-ca-tra. Accessed: January, 2022. [in Vietnamese]
Singh P., Benjakul S., Maqsood S., Kishimura H., 2011 Isolation and characterisation of collagen extracted from the skin of striped catfish (*Pangasianodon hypophthalmus*). Food Chemistry 124:97-105.
Thomas V., Dean D. R., Jose M. V., Mathew B., Chowdhury S., Vohra Y. K., 2007 Nanostructured biocomposite scaffolds based on collagen coelectrospun with nanohydroxyapatite. Biomacromolecules 8(2):631-637.
Tiktopulo E. I., Kajava A. V., 1998 Denaturation of type I collagen fibrils is an endothermic process accompanied by a noticeable change in the partial heat capacity. Biochemistry 37(22):8147-8152.
Trelstad R. L., Hayashi K., Gross J., 1976 Collagen fibrillogenesis: intermediate aggregates and suprafibrillar order. Proceedings of the National Academy of Sciences of the USA 73(11):4027-4031.
Uquillas J. A., Kishore V., Akkus O., 2011 Effects of phosphate-buffered saline concentration and incubation time on the mechanical and structural properties of electrochemically aligned collagen threads. Biomedical Materials 6(3):035008.
Venugopal J., Low S., Choon A. T., Sampath Kumar T. S., Ramakrishna S., 2008 Mineralization of osteoblasts with electrospun collagen/hydroxyapatite nanofibers. Journal of Materials Science: Materials in Medicine 19(5):2039-2046.
Wang L., Liang Q., Chen T., Wang Z., Xu J., Ma H., 2014 Characterization of collagen from the skin of Amur sturgeon (*Acipenser schrenckii*). Food Hydrocolloids 38(3): 104-109.
Wei G., Ma P. X., 2004 Structure and properties of nano-hydroxyapatite/polymer composite scaffolds for bone tissue engineering. Biomaterials 25(19):4749-4757.
Zhang X., Ookawa M., Tan Y., Ura K., Adachi S., Takagi Y., 2014 Biochemical characterisation and assessment of fibril-forming ability of collagens extracted from Bester sturgeon *Huso huso* x *Acipenser ruthenus*. Food Chemistry 160:305-312.
Zhu J., Kaufman L. J., 2014 Collagen I self-assembly: revealing the developing structures that generate turbidity. Biophysical Journal 106(8):1822-1831.
Zhuang H., Zheng J. P., Gao H., De Yao K., 2007 *In vitro* biodegradation and biocompatibility of gelatin/montmorillonite-chitosan intercalated nanocomposite. Journal of Materials Science: Materials in Medicine 18(5):951-957.

Received: 08 June 2022. Accepted: 06 July 2022. Published online: 30 July 2022.
Authors:
Quoc Phong Ho, College of Engineering Technology, Can Tho University, 3/2 Street, Ninh Kieu District, Can Tho City 94115, Vietnam, e-mail: hqphong@ctu.edu.vn
Minh Thuy Le Thi, College of Aquaculture and Fisheries, Can Tho University, 3/2 Street, Ninh Kieu District, Can Tho City 94115, Vietnam, e-mail: ltmthuy@ctu.edu.vn
Lien Huong Huynh, College of Engineering Technology, Can Tho University, 3/2 Street, Ninh Kieu District, Can Tho City 94115, Vietnam, e-mail: hlhuong@ctu.edu.vn
Minh Phu Tran, College of Aquaculture and Fisheries, Can Tho University, 3/2 Street, Ninh Kieu District, Can Tho City 94115, Vietnam, e-mail: tmphu@ctu.edu.vn
Bich Thuyen Nguyen Thi, College of Engineering Technology, Can Tho University, 3/2 Street, Ninh Kieu District, Can Tho City 94115, Vietnam, e-mail: ntbthuyen@ctu.edu.vn
Yasuaki Takagi, Faculty of Fisheries Sciences, Hokkaido University, 3-1-1 Minatocho, Hakodate, Hokkaido 041-8611, Japan, e-mail: takagi@fish.hokudai.ac.jp

How to cite this article:
Ho Q. P., Thi M. T. L., Huynh L. H., Tran M. P., Thi B. T. N., Takagi Y., 2022 Preparation of collagen nanofibril-scaffold from the skin of catfish (*Pangasianodon hypophthalmus*) farmed in the Mekong Delta. AACL Bioflux 15(4):1850-1860.